Biochem. J. (1987) 244, 165–171 (Printed in Great Britain)

Kinetics of carbonyl reductase from human brain

Kurt M. BOHREN, Jean-Pierre VON WARTBURG and Bendicht WERMUTH*
Institut für Biochemie und Molekularbiologie der Universität Bern, Bühlstrasse 28, CH-3012 Berne, Switzerland

Initial-rate analysis of the carbonyl reductase-catalysed reduction of menadione by NADPH gave families of straight lines in double-reciprocal plots consistent with a sequential mechanism being obeyed. The fluorescence of NADPH was increased up to 7-fold with a concomitant shift of the emission maximum towards lower wavelength in the presence of carbonyl reductase, and both NADPH and $NADP^+$ caused quenching of the enzyme fluorescence, indicating formation of a binary enzyme–coenzyme complex. Deuterium isotope effects on the apparent V/K_m values decreased with increasing concentrations of menadione but were independent of the NADPH concentration. The results, together with data from product inhibition studies, are consistent with carbonyl reductase obeying a compulsory-order mechanism, NADPH binding first and $NADP^+$ leaving last. No significant differences in the kinetic properties of three molecular forms of carbonyl reductase were detectable.

INTRODUCTION

Carbonyl reductase (EC 1.1.1.184) is a cytosolic monomeric oxidoreductase that catalyses the NADPH-dependent reduction of a variety of quinones and other carbonyl compounds to the corresponding quinols and alcohol products. Multiple forms of the enzyme differing in size and charge have been isolated from various sources (for review see [1]). Three forms of the enzyme have been purified from human brain [2]. Together with aldehyde reductase (EC 1.1.1.2) and aldose reductase (EC 1.1.1.21), carbonyl reductase constitutes the enzyme family of the aldo–keto reductases in human and other mammalian tissues [1,3]. This grouping into an enzyme family is based on similar physicochemical properties and a broad overlapping substrate specificity, but has little additional corroboration. In order to characterize and compare further the three reductases from human tissues, an investigation of the kinetic mechanism was initiated. Results of these studies with aldehyde reductase and aldose reductase have been published [4,5]. We here report the results of a study on the kinetic mechanism of carbonyl reductase from human brain. The present data are in agreement with a compulsory-order mechanism in which NADPH binds to the enzyme first.

EXPERIMENTAL

Materials

Carbonyl reductase from human brain was purified and the molecular forms, named according to their isoelectric points as CR_7, CR_8 and $CR_{8.5}$ respectively, were separated as described previously [2]. All three forms were homogeneous as judged by SDS/polyacrylamide-gel electrophoresis and polyacrylamide-gel isoelectric focusing. Horse liver alcohol dehydrogenase and bovine liver glutamate dehydrogenase were obtained from Boehringer (Mannheim, Germany). L-[U-$^2H_5$ (non-labile protons)]Glutamic acid was purchased from C.E.A. (Saclay, France), and [$^2H_6$]ethanol was obtained from Merck (Darmstadt, Germany). Nicotinamide nucleotides were purchased from Sigma Chemical Co. (St. Louis, MO, U.S.A.). All other chemicals including menadione were obtained from Fluka (Buchs, Switzerland) and Merck, and were of the highest grade available. Menadione, which was not sufficiently soluble in water, was dissolved in methanol. The final concentration of the alcohol did not exceed 0.1% and had no effect on the catalytic activity of carbonyl reductase. DEAE-Sepharose was purchased from Pharmacia (Uppsala, Sweden).

Preparation of (4*S*)-[4-^{2}H]NADPH and (4*R*)-[4-^{2}H]NADPH

Carbonyl reductase catalyses the transfer of the pro-4*S*-hydrogen atom of the nicotinamide ring of NADPH to the carbonyl substrate [2]. Appropriately labelled (4*S*)-[4-^{2}H]NADPH was prepared by adding bovine liver glutamate dehydrogenase (10 units/ml of reaction mixture) to a solution consisting of 1.6 mM-$NADP^+$ and 6.5 mM-L-[U-$^2H_5$]glutamic acid in 0.1 M-sodium phosphate buffer, pH 8.0. The mixture was incubated for 1 h at 25 °C, then 5 ml portions were loaded on to DEAE-Sepharose columns (1 cm × 10 cm) equilibrated with water. The columns were developed with increasing concentrations of $(NH_4)HCO_3$ at 4 °C. The labelled coenzyme was eluted at approximately 0.25 M-$(NH_4)HCO_3$. Fractions exhibiting an A_{260}/A_{340} ratio less than 2.4:1 were combined and used directly for kinetic experiments within 10 h.

(4*R*)-[4-^{2}H]NADPH, which was used as a control, was prepared similarly by adding horse liver alcohol dehydrogenase (2 units/ml of reaction mixture) to a solution containing 2 mM-$NADP^+$, 35 mM-[$^2H_6$]ethanol, 40 mM-semicarbazide hydrochloride and 1 mM-EDTA in 0.1 M-sodium pyrophosphate buffer, pH 8.8. The mixture was incubated for 2 h at 25 °C and the labelled NADPH was purified as described above.

Enzyme assay and kinetic measurements

Reaction mixtures consisted of 100 mM-sodium phosphate buffer, pH 7.0, containing NADPH or (4*S*)-[4-^{2}H]NADPH or (4*R*)-[4-^{2}H]NADPH, menadione and

* To whom correspondence should be addressed.

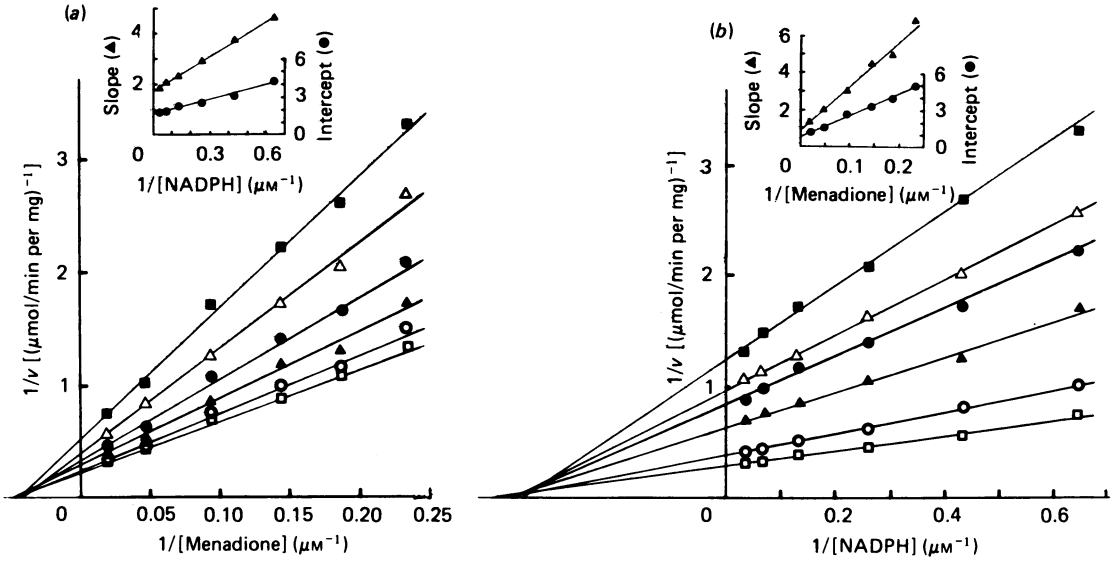

Fig. 1. Double-reciprocal plots from initial-rate measurements of the reduction of menadione by NADPH catalysed by carbonyl reductase (CR_8)

Details of the assay procedure were as described in the text. (*a*) The NADPH concentrations were 1.6 μM (■), 2.3 μM (△), 3.9 μM (●), 7.8 μM (▲), 15.6 μM (○) and 31.3 μM (□). (*b*) The menadione concentrations were 4.3 μM (■), 5.4 μM (△), 7.0 μM (●), 10.7 μM (▲), 21.4 μM (○) and 53.6 μM (□). The insets show replots of slopes and intercepts versus the reciprocal of the concentration of the fixed-concentration substrate. Slope and intercept values are in arbitrary units.

product inhibitor ($NADP^+$) as specified in the Results section in a total volume of 1.0 ml. Reactions were started by the addition of enzyme, and the decrease in A_{340} was monitored at 25 °C. Initial rates were measured in triplicate for 1–2 min. Controls lacking either substrate or enzyme were routinely included. Accurate concentrations of menadione, NADPH or ^{2}H-labelled NADPH, and $NADP^+$ were determined spectrophotometrically at 333, 340 and 260 nm, assuming molar absorption coefficients of 2500, 6300 and 18000 $M^{-1} \cdot cm^{-1}$ respectively. NADPH was dissolved in 50 mM-sodium phosphate buffer, pH 8.0, and kept at 0 °C to prevent degradation. In the isotopic experiments NADPH was dissolved in 0.25 M-$(NH_4)HCO_3$. The ionic strength and pH of the reaction mixtures were held constant by adding appropriate amounts of $(NH_4)HCO_3$ (maximal increase in pH was 0.1). One enzyme unit is defined as the change in absorbance at 340 nm corresponding to the oxidation of 1 μmol of NADPH/min.

Protein concentration

The concentration of carbonyl reductase was determined by using the Bio-Rad Protein Assay Kit, with bovine γ-globulin as standard.

Kinetic analysis

Initial-rate data were fitted by non-linear regression in accordance with Wilkinson [6], and results are presented as double-reciprocal plots for illustrative purposes. Lines in secondary plots of these data were fitted by linear regression. Rate equations (see the Results section) were fitted to the experimental data by using a simplex algorithm [7], and the adequacy of the applied equation was verified by Monte Carlo sensitivity analysis [7]. For each analysis 25 data sets were simulated and a 95% level of significance ($\alpha = 0.05$) based on a t distribution was applied. This method also provided estimates of the standard deviation of the computed parameters. Apparent isotope effects were determined by taking the ratio of intercepts (^DV) and slopes [$^D(V/K_m)$] of double-reciprocal plots obtained with deuterated and non-deuterated NADPH.

Binding studies

Spectrophotometric measurements were performed on a Perkin–Elmer double-beam spectrophotometer (model 555) at 20 °C. Increasing concentrations of NADPH or $NADP^+$ (0.2–20 μM) were added to carbonyl reductase (3.5–5.5 nmol/ml of 50 mM-sodium phosphate buffer, pH 7.5), and the absorbance between 240 and 400 nm was recorded and corrected for the contribution by the enzyme protein. Fluorescence titration experiments were carried out on a Perkin–Elmer MPF-2A fluorimeter with 1 cm quartz cuvettes. All experiments were performed in 50 mM-sodium phosphate buffer, pH 7.5, at 10 °C. Binding of coenzyme was monitored by the enhancement of NADPH fluorescence (excitation at 345 nm, emission at 448 nm) and by the quenching of protein fluorescence (excitation at 290 nm, emission at 335 nm). In a typical binding experiment 1.7 ml each of enzyme solution (3.5–5.5 μM) and reference buffer were titrated with a coenzyme stock solution (1.2–1.4 mM), with a total volume of 40–50 μl, and the relative intensity of fluorescence was measured for 5 s. In order to minimize side effects from destruction of coenzyme under assay conditions, a titration experiment consisting of 12 additions was completed within 10 min. Data were corrected for primary inner-filter effects by the method of Malencik & Anderson [8] and treated as described by Luisi and colleagues [9,10], assuming that only enzymically active enzyme was able to bind coenzyme. Dissociation constants were calculated from Hill plots with the use of linear-regression analysis.

Table 1. Kinetic constants of carbonyl reductase from human brain

		$CR_{8.5}$	CR_8	CR_7
K_s^{NADPH} (μM)		2.7±0.3	2.7±0.4	3.0±0.3
K_m^{NADPH} (μM)		3.6±0.3	2.2±0.2	2.0±0.2
$K_m^{menadione}$ (μM)		27±3	21±2	23±2
V (μmol/min per mg)		5.8±0.3	4.8±0.3	2.3±0.2
$K_{ic}^{NADP^+}$* (μM)	[NADPH] varied†	6.4±1.1	5.5±0.4	3.9±1.0
	[NADPH] varied‡	–	8.5±1.1	–
	[Menadione] varied§	93±14	73±3	63±4
$K_{iu}^{NADP^+}$(μM)	[Menadione] varied§	168±15	155±3	155±15

* In the ordered Bi Bi mechanism $K_{ic}^{NADP^+}$ ([NADPH] varied) corresponds to $K_s^{NADP^+}$.
† Menadione concentration 241 μM.
‡ Menadione concentration 11 μM.
§ NADPH concentration 61 μM.

RESULTS

Initial-velocity studies

When menadione was the varied-concentration substrate and NADPH concentration was held constant, double-reciprocal plots of initial velocity against menadione concentration yielded a family of straight lines intersecting to the left of the ordinate (Fig. 1*a*). When NADPH was the varied-concentration substrate and menadione concentration was kept constant, double-reciprocal plots of initial velocity against NADPH again gave intersecting lines (Fig. 1*b*). Replots of the slopes and intercepts against the reciprocal of the fixed substrate concentration for each of these experiments were linear (insets to Figs. 1*a* and 1*b*). These results are indicative of a sequential mechanism. Assuming steady-state conditions and an ordered addition of substrates, NADPH binding first, this mechanism is described by eqn. (1) [11]:

$$v = V[A][B]/(K_s^A K_m^B + K_m^B[A] + K_m^A[B] + [A][B]) \quad (1)$$

where [A] and [B] represent the concentrations of NADPH and menadione respectively and K_m^A and K_m^B are the respective limiting Michaelis constants. K_s^A is the equilibrium dissociation constant of the binary enzyme–NADPH complex assuming that this complex undergoes no transformation before the binding of menadione. Numeric values of V, K_m^A, K_m^B and K_s^A were determined for all three forms of carbonyl reductase and are listed in Table 1.

Product inhibition studies

When NADPH was the varied-concentration substrate and menadione concentration was held constant at near-saturating (241 μM) and non-saturating concentrations (11 μM), $NADP^+$ gave linear competitive-inhibition patterns, as shown for the higher menadione concentration in Fig. 2(*a*). When NADPH concentration was kept constant at 61 μM and menadione was the varied-concentration substrate, linear mixed inhibition was obtained with $NADP^+$ (Fig. 2*b*). In both cases replots of slopes and intercepts were linear. These inhibition patterns are described by eqns. (2) and (3) [12]:

$$v = V[A]/\{K_m^A(1 + [i]/K_{ic}) + [A]\} \quad (2)$$

$$v = V[B]/\{K_m^B(1 + [i]/K_{ic}) + [B](1 + [i]/K_{iu})\} \quad (3)$$

where K_{ic} and K_{iu} represent the competitive and uncompetitive inhibition constants for $NADP^+$ with respect to NADPH (eqn. 2) and menadione (eqn. 3) and [i] is the concentration of $NADP^+$. V, K_m^A and K_m^B have the same meaning as in eqn. (1), but they become apparent values at non-saturating concentrations of the fixed substrate. Numeric values of K_i were obtained by fitting the two equations to the experimental data and are given in Table 1 for all three enzyme forms.

The initial-velocity patterns, together with the inhibition patterns, are consistent with an ordered addition of substrates, NADPH binding first, although other sequential mechanisms in which menadione binds first or with random addition of substrates cannot be excluded. For a more definite discrimination between different mechanisms it would be necessary to obtain the inhibition patterns with the quinol product and to carry out kinetic studies in the reverse direction. However, the extreme instability of menadiol precluded these experiments. Alternative alcohol products of known substrates of carbonyl reductase were essentially inactive as inhibitors. In order to elucidate further the kinetic mechanism of carbonyl reductase, substrate-binding and isotope-effect studies were carried out.

Isotope effects

For the purpose of determining the order of addition of reactants in a bi-reactant mechanism, we can employ Scheme 1 [13], in which only k_{+5} is isotope-sensitive. k_{+5} includes all of the steps that the initially formed EAB complex undergoes, up to and including the release of the first product. The constant k_{+6} then includes release of the second product and any other step (such as isomerization of EQ) that limits V, but not V/K_m, for either substrate. Isotope effects on V depend on both k_{+5} and k_{+6} and are described by the same equation regardless of the order or randomness of substrate addition [13]. Variations in ^DV at various concentrations of the fixed-concentration substrate, however, allow certain conclusions concerning the location and degree of rate limitation of the isotope-sensitive step(s). The effect of increasing concentrations of menadione at infinite concentrations of NADPH/(4*S*)-[4-^{2}H]NADPH on ^DV is shown in Table 2. A similar inverse relationship was obtained when NADPH/(4*S*)-[4-^{2}H]NADPH was the

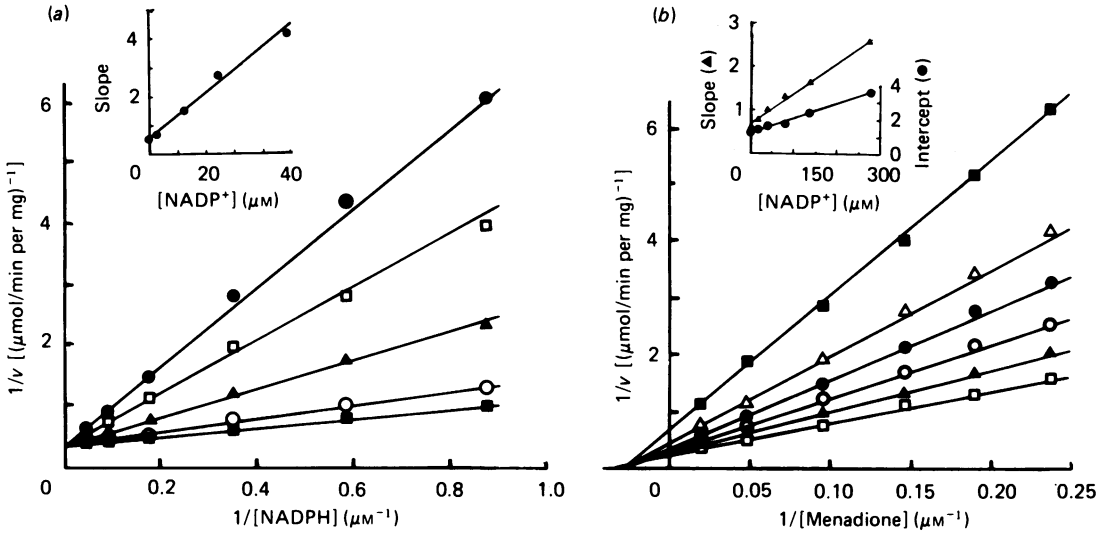

Fig. 2. Inhibition of carbonyl reductase (CR_8) by $NADP^+$ with respect to NADPH (*a*) and menadione (*b*)

The concentration of the fixed-concentration substrate was 241 μM-menadione in (*a*) and 61 μM-NADPH in (*b*). $NADP^+$ concentrations were: (*a*) 0 μM (■), 2.5 μM (○), 12.3 μM (▲), 24.2 μM (□) and 48.4 μM (●); (*b*) 0 μM (□), 15.7 μM (▲), 39.3 μM (○), 78.7 μM (●), 137 μM (△) and 274 μM (■). Slope and intercept values in the insets are in arbitrary units.

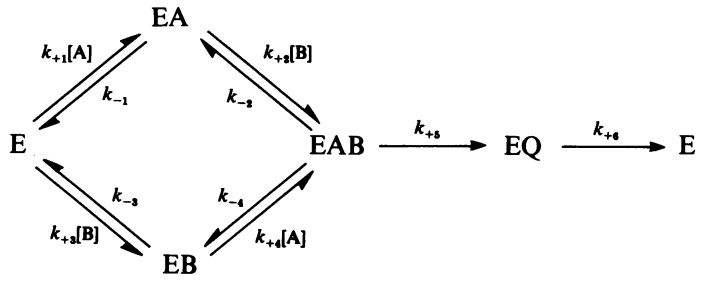

Scheme 1.

fixed-concentration substrate, although the isotope effect did not fall below 1.2 at saturating concentrations of NADPH/(4*S*)-[4-^{2}H]NADPH. The results indicate that other steps than k_{+5}, such as the release of $NADP^+$, are partially rate-limiting. No isotope effects were detectable when (4*R*)-[4-^{2}H]NADPH was used instead of (4*S*)-[4-^{2}H]NADPH.

In contrast with ^DV, isotope effects on V/K_m depend on the kinetic mechanism. For the compulsory-order mechanism with two substrates (ordered Bi Bi) in which k_{+3}, k_{-3}, k_{+4} and k_{-4} of Scheme 1 are zero the following equations apply [13]:

$$^D(V/K_m^B) = (^Dk + K_1)/(1 + K_1) \quad (4)$$

$$^D(V/K_m^A) = \{^Dk + K_1(1 + K_2[B])\}/\{1 + K_1(1 + K_2[B])\} \quad (5)$$

where ^Dk is the isotope effect on the rate constant for the isotope-sensitive step, K_1 the k_{+5}/k_{-2} ratio and K_2 the k_{+2}/k_{-1} ratio. Eqn. (4) predicts that an isotope effect on V/K_m^B will be seen at any concentration of substrate A (NADPH), whereas from eqn. (5) it follows that the isotope effect on V/K_m^A will disappear at infinite concentrations of substrate B (menadione), but become equal to $^D(V/K_m^B)$ as the concentration of B goes to zero. The experimental values of $^D(V/K_m^A)$ and $^D(V/K_m^B)$ at various concentrations of menadione and NADPH/^{2}H-labelled NADPH respectively are shown in Fig. 3.

Table 2. Deuterium isotope effect on $V^{app.}$ (^DV) as a function of the concentration of menadione

[Menadione] (μM)	^DV (μmol/min per mg)
12	2.37±0.17
25	2.11±0.11
39	1.77±0.14
103	1.40±0.06
250	1.05±0.08

Fitting eqn. (5) to the experimental data yielded the following values for ^Dk, K_1 and K_2: $^Dk = 3.6 \pm 0.7$, $K_1 = 0.31 \pm 0.18$ and $K_2 = 0.15 \pm 0.06$.

Binding studies

No change in the absorption spectrum of NADPH in the range of the absorbance maxima at 260 and 340 nm was detectable in the presence of carbonyl reductase. Similarly, the spectrum of $NADP^+$ remained unchanged in the presence of carbonyl reductase, nor were we able to detect any additional absorbance above 300 nm (Racker band) in the presence of the protein [14].

However, measurements of both NADPH and enzyme

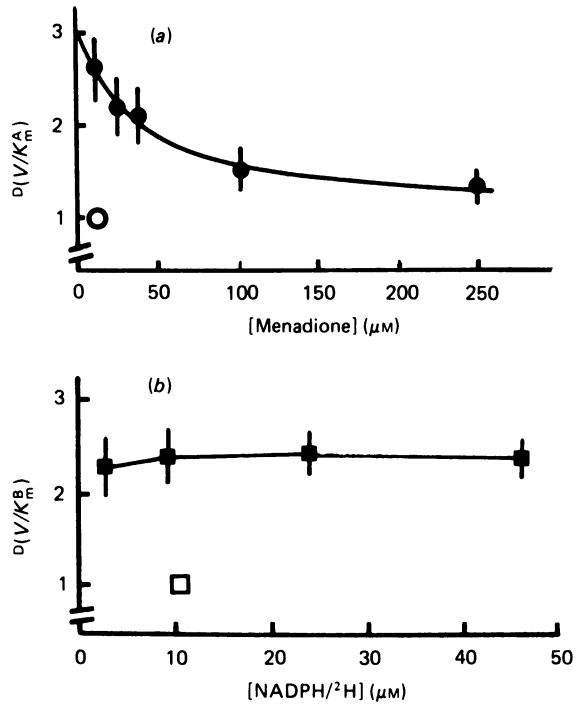

Fig. 3. Deuterium isotope effect on V/K_m [$^{D}(V/K_m)$] as a function of the concentration of the fixed-concentration substrate

$^{D}(V/K_m)$ values were obtained from the ratio of slopes of double-reciprocal plots of initial rates versus the concentration of the coenzyme (2–20 μM) and menadione (8–70 μM) respectively, with deuterated and unlabelled NADPH. One point thus represents a data set of at least 20 initial-rate measurements. The curve in (*a*) represents the best fit obtained by using eqn. (5). Controls (○ and □) were measured with (4*R*)-[4-^{2}H]NADPH.

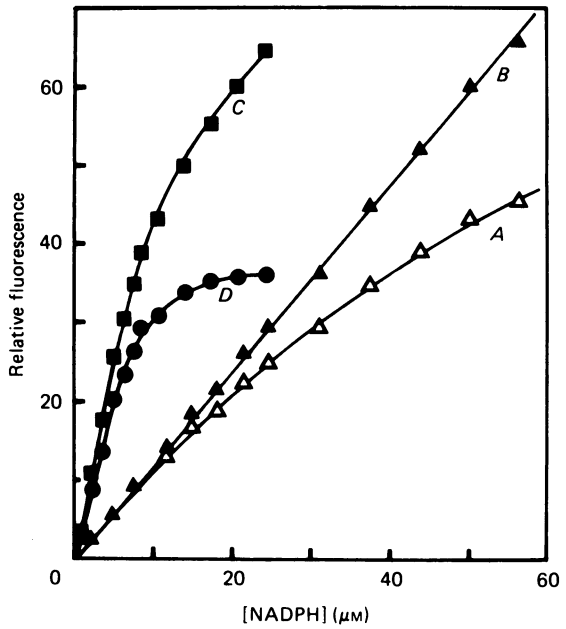

Fig. 4. Fluorescence enhancement of NADPH by carbonyl reductase

Calibration curves in the absence of enzyme (curve *A*) uncorrected and (curve *B*) corrected for primary inner-filter effects. Curve *C*, corrected curve in the presence of enzyme. Curve *D*, titration curve representing the difference between curves *C* and *B*. Experimental conditions were as described in the Experimental section. Ordinate values are relative fluorescence. The initial concentration of enzyme (CR_8) was 5.5 μM.

fluorescence gave evidence of the formation of a binary enzyme–coenzyme complex. The fluorescence of NADPH was increased in the presence of carbonyl reductase and the fluorescence emission maximum was shifted from 456 to 445 nm. Titration of the enzyme with NADPH gave a typical saturation curve (Fig. 4), from which we extrapolated a maximum fluorescence increase, $\Delta F_{max.}$, of 7-fold (corresponding to the ordinate intercept in a double-reciprocal plot of the peak height of relative NADPH fluorescence versus the concentration of bound NADPH) and a dissociation constant for NADPH of 2.4±0.4 μM (Fig. 5*a*).

Addition of both NADPH and $NADP^+$ to carbonyl reductase decreased the enzyme's intrinsic fluorescence, but did not affect the wavelength of the emission maximum at 335 nm. Titration curves of the decrease in fluorescence versus the nucleotide concentration again followed saturation kinetics, yielding dissociation constants for NADPH and $NADP^+$ of 1.5±0.4 μM and 1.0±0.5 μM respectively, as shown for $NADP^+$ in Fig. 5(*b*).

Interaction between carbonyl reductase and NADPH was further demonstrated by the transfer of energy between the enzyme protein and the coenzyme, in that excitation of the enzyme at 290 nm in the presence of NADPH caused the coenzyme to emit light at 445 nm. Controls containing only enzyme or coenzyme showed no fluorescence at 445 nm. From these experiments a dissociation constant for the enzyme–NADPH complex of 2.0±0.4 μM was extrapolated, in good agreement with the values obtained from the fluorescence enhancement of NADPH and the fluorescence quenching of the enzyme.

DISCUSSION

The intersecting lines obtained in the initial-velocity studies in the absence of products are consistent with a sequential kinetic mechanism and rule out a mechanism involving a substituted enzyme (double-displacement of ping-pong mechanism), which yields parallel lines in a double-reciprocal plot [11]. Similarly, a steady-state random mechanism seems unlikely, since this mechanism yields non-linear double-reciprocal plots, although deviations from linearity may not always be evident [15]. Further discrimination between other feasible mechanisms was made possible by the results of the product inhibition studies. The data rule out a rapid-equilibrium random mechanism (without formation of dead-end complexes), which, in contrast with the observed mixed inhibition pattern (Fig. 2*b*), would yield competitive inhibition by $NADP^+$ with respect to menadione. Moreover, a distinction between the ordered and the rapid-equilibrium random mechanisms is possible on the basis of the inhibition constants for $NADP^+$ with respect to NADPH at different concentrations of menadione. In the rapid-equilibrium random mechanism this constant increases with the concentration of the fixed substrate,

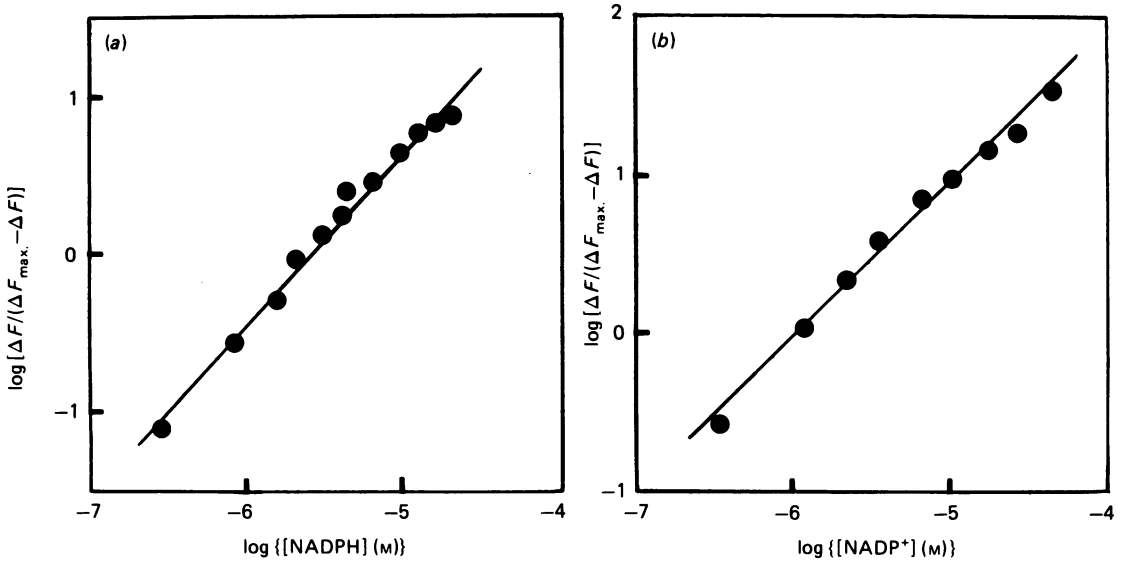

Fig. 5. Hill plots of NADPH and NADP$^+$ binding to carbonyl reductase

(*a*) Data were obtained from NADPH fluorescence enhancement based on the titration curve in Fig. 3. (*b*) Data were obtained from enzyme fluorescence quenching by NADP$^+$ as described in the text ([CR_8] = 4.1 μM). ΔF and $\Delta F_{max.}$ are the actual and maximum relative fluorescence changes respectively.

whereas in the ordered mechanism it remains constant. The similar values obtained at 11 μM- and 241 μM-menadione (Table 1) do not support the rapid-equilibrium random mechanism.

For the ordered Bi Bi mechanism K_s^Q, the dissociation constant of the binary enzyme–NADP$^+$ complex, equals the inhibition constant K_{ic} for NADP$^+$ with respect to NADPH (eqn. 2). On the other hand, K_s^Q is also related to the inhibition constants K_{ic} and K_{iu} for NADP$^+$ with respect to menadione (eqn. 3) by the following relationships [12]:

$$K_{ic} = K_s^Q(1+[A]/K_s^A) \quad (6)$$
$$K_{iu} = K_s^Q(1+[A]/K_m^A) \quad (7)$$

Substituting the values for K_{ic} and K_{iu} of CR_8 from Table 1 into eqns. (6) and (7) gives values for K_s^Q of 3.1 ± 0.5 μM and 5.4 ± 0.5 μM, in good agreement with the value of 5.5 ± 0.5 μM determined directly (Table 1). Values that agreed well were also obtained with the two other molecular forms of the enzyme.

The product inhibition patterns also give further evidence against the steady-state random Bi Bi mechanism, which allows no competitive inhibition. On the other hand, in addition to a compulsory-order mechanism in which NADPH binds to the enzyme first, the results from the product inhibition studies are also consistent with a mechanism in which menadione binds to the enzyme first and in which the steps describing the formation, conversion and dissociation of the central EAB/EPQ complex are kinetically not significant (Theorell–Chance mechanism), and with a rapid-equilibrium random Bi Bi mechanism in which NADP$^+$, menadione and the enzyme combine to form a dead-end complex. The Theorell–Chance mechanism, however, is excluded by the data from the binding experiments, which showed that both NADPH and NADP$^+$ bind to the free enzyme. The rapid-equilibrium random mechanism with formation of an EBQ dead-end complex, finally, may be rejected on the basis of the results from the isotope studies. In the ordered mechanism, increasing the concentration of substrate B drives the binary EA complex into the ternary central complex, and, in doing so, raises the commitment to catalysis of the EA complex to infinity. Hence, as the concentration of B goes to infinity, the isotope effect on V/K_m^A becomes unity. In the rapid-equilibrium random mechanism all substrates are released from the enzyme much faster than they are converted into products, resulting in a very low commitment to catalysis. Consequently, the isotope effects on V/K_m^A and V/K_m^B are identical regardless of the concentration of the fixed-concentration substrate. As shown in Fig. 3, $^D(V/K_m^{NADPH})$ clearly varied with the concentration of menadione. Thus the results from the initial-velocity, product inhibition, substrate-binding and isotope-effect studies are consistent with the assumption that carbonyl reductase from human brain operates by an ordered Bi Bi mechanism in which the coenzyme binds to the enzyme first.

This type of mechanism is common among nicotinamide nucleotide-dependent dehydrogenases, and has also been observed with aldo–keto reductases. Both aldehyde reductase and aldose reductase from human tissues follow compulsory-order mechanisms in which NADPH binds to the enzyme first [4,5]. Similarly, ordered binding of NADPH and aldehyde substrate was observed with aldehyde reductase from various other species (for review see [16]), although a certain randomness of substrate addition may occur with some aldehydes. Thus aldehyde reductase from pig liver followed an ordered Bi Bi mechanism with pyridine-3-aldehyde as substrate, but a partially random mechanism with *p*-carboxybenzaldehyde as substrate [17]. Results obtained from kinetic studies with aldose reductase have been conflicting, and both ordered [5,18,19] and random mechanisms [20,21] have been proposed. Evidence has recently been presented that in some tissues aldose reductase occurs in two molecular forms with different enzymic properties [22], which may explain many of the controversial findings with this enzyme. The present study showed that all three forms of carbonyl reductase obey the same

kinetic mechanism and differ only slightly in their kinetic constants, indicating that the structural differences do not affect the kinetic properties.

The phenomena observed with carbonyl reductase in the spectrofluorimetric studies, i.e. the enhancement of NADPH fluorescence with a concomitant blue-shift of the emission maximum as well as the quenching of the protein fluorescence upon formation of a binary complex, are also quite common among dehydrogenases, and likewise have been observed with aldehyde reductase from pig tissues [23,24]. Using methods based on the spectrofluorimetric changes, we have obtained dissociation constants for the binary NADPH–protein complex (K_s^{NADPH}) that are identical within experimental error (2.4 ± 0.4, 1.5 ± 0.4 and 2.0 ± 0.4 μM) and also closely agree with the value of 2.7 ± 0.4 μM determined kinetically. Somewhat less agreement between the kinetically and spectrofluorimetrically determined values was obtained for the dissociation constant for $NADP^+$ ($K_s^{NADP^+}$). However, the experimental conditions differed slightly in the kinetic and spectrofluorimetric experiments, which may have had a greater effect on $K_s^{NADP^+}$ than on K_s^{NADPH}.

Both aldehyde reductase [24–26] and aldose reductase [27,28] from various tissues cause a marked red-shift of the NADPH absorption maximum at 340 nm upon formation of a binary complex. In contrast, in the present study no change in the absorption spectrum of NADPH was detectable after binding to carbonyl reductase. Since spectral shifts are generally associated with changes in the polarity of the surrounding environment, sizable structural differences between the coenzyme-binding domain of carbonyl reductase and the other aldo–keto reductases may be expected. Structurally different coenzyme binding sites are also reflected by the stereospecificity of hydrogen transfer of the three enzymes. Aldehyde reductase and aldose reductase catalyse the transfer of the pro-(4*R*)-hydrogen atom of NADPH, whereas carbonyl reductase is a B-side-specific enzyme [1–3].

In summary, carbonyl reductase from human brain exhibits many characteristics common to nicotinamide nucleotide-dependent dehydrogenases, including aldehyde reductase and aldose reductase, but seems to differ from these two members of the aldo–keto reductase family with respect to the architecture of the active site.

This work was supported by a grant from the Swiss National Science Foundation.

Received 28 November 1986; accepted 27 January 1987

REFERENCES

1. Wermuth, B. (1985) in Enzymology of Carbonyl Metabolism 2 (Flynn, T. G. & Weiner, H., eds.), pp. 209–230, Alan R. Liss, New York
2. Wermuth, B. (1981) J. Biol. Chem. **256**, 1206–1213
3. Wermuth, B. (1982) in Enzymology of Carbonyl Metabolism (Weiner, H. & Wermuth, B., eds.), pp. 261–274, Alan R. Liss, New York
4. Wermuth, B. & von Wartburg, J.-P. (1980) in Alcohol and Aldehyde Metabolizing Systems 4 (Thurman, R. G., ed.), pp. 189–195, Plenum Press, New York
5. Wermuth, B., Bürgisser, H. P., Bohren, K. & von Wartburg, J.-P. (1982) Eur. J. Biochem. **127**, 279–284
6. Wilkinson, G. N. (1961) Biochem. J. **80**, 324–332
7. Caceci, M. S. & Cacheris, W. P. (1984) Byte **5**, 340–362
8. Malencik, D. A. & Anderson, S. R. (1972) Biochemistry **11**, 2766–2771
9. Luisi, P. L. & Favilla, R. (1970) Eur. J. Biochem. **17**, 91–94
10. Luisi, P. L., Olomucki, A., Baici, A. & Karlovic, D. (1973) Biochemistry **12**, 4100–4106
11. Cleland, W. W. (1963) Biochim. Biophys. Acta **67**, 104–137
12. Cleland, W. W. (1963) Biochim. Biophys. Acta **67**, 173–187
13. Cook, P. F. & Cleland, W. W. (1981) Biochemistry **20**, 1790–1796
14. Racker, E. & Krimsky, I. (1952) J. Biol. Chem. **198**, 731–743
15. Pettersson, G. (1970) Acta Chem. Scand. **24**, 1271–1279
16. Tipton, K. F. (1982) in Enzymology of Carbonyl Metabolism (Weiner, H. & Wermuth, B., eds.), pp. 197–208, Alan R. Liss, New York
17. Magnien, A. & Branlant, G. (1983) Eur. J. Biochem. **131**, 375–381
18. Boghosian, R. A. & McGuinness, E. T. (1981) Int. J. Biochem. **13**, 909–914
19. Ryle, C. M. & Tipton, K. F. (1985) Biochem. J. **227**, 621–627
20. Halder, A. B. & Crabbe, M. J. C. (1984) Biochem. J. **219**, 33–39
21. Doughty, C. C. & Conrad, S. M. (1982) Biochim. Biophys. Acta **708**, 358–364
22. Das, B. & Srivastava, S. K. (1985) Diabetes **34**, 1145–1151
23. Flynn, T. G., Shires, J. & Walton, D. J. (1975) J. Biol. Chem. **250**, 2933–2940
24. Morpeth, F. F. & Dickinson, F. M. (1980) Biochem. J. **191**, 619–626
25. Wermuth, B., Münch, J. D. B. & von Wartburg, J.-P. (1977) J. Biol. Chem. **252**, 3821–3828
26. Branlant, G. & Biellmann, J.-F. (1980) Eur. J. Biochem. **105**, 611–621
27. Branlant, G. (1982) Eur. J. Biochem. **129**, 99–104
28. Cromlish, J. A. & Flynn, T. G. (1983) J. Biol. Chem. **258**, 3416–3424